

APPLICATION OF DIGITAL MARKER EXTENSOMETRY TO DETERMINE THE TRUE STRESS-STRAIN BEHAVIOR OF IRRADIATED METALS AND ALLOYS - M. N. Gusev, O. P. Maksimkin, I. S. Osipov (Institute of Nuclear Physics, Almaty, Kazakhstan) and F. A. Garner (Pacific Northwest National Laboratory, Richland WA USA)

OBJECTIVE

The object of this effort is to develop experimental tools to better understand the origin and parametric dependencies of radiation-induced changes in mechanical properties of structural steels used in reactor construction.

SUMMARY

To study the mechanisms of deformation hardening and flow localization of radioactive materials, a non-contact “digital marker extensometry” technique has been employed. It allows researchers to easily define plasticity parameters and true stresses in experiments where highly radioactive miniature specimens are used.

The engineering and “true stress – true local strain” relationships of irradiated metal polycrystals during plastic flow and hardening have been investigated experimentally after irradiation in two reactors in Kazakhstan. The true curves were obtained for copper, nickel, iron, molybdenum, as well as for the Russian stainless steels 08Cr16Ni11Mo3 and 12Cr18Ni10Ti. Describing these curves using the equation $\sigma_i = \sigma_0 + k\sqrt{\varepsilon_i}$ demonstrates that the concept of ultimate stress in highly irradiated materials is an artifact arising from flow localization and is not fully informative of the operating hardening mechanisms.

PROGRESS AND STATUS

Introduction

To describe the plastic deformation behavior of polycrystalline metals, it is necessary to utilize dislocation theory [1, 2] combined with elements of thermodynamics [3] and mesomechanics [4]. In some cases, material-specific physical processes involved in plastic flow also need to be taken into account. Examples of such processes are interrupted deformation (dynamic strain aging) [5], microscopic or macroscopic flow localization [1, 2], arising from defect-dislocation interactions, particularly from defects induced by displacive radiation [6].

In such cases the “true” curves of deformation hardening expressed in true stress-true local strain coordinates are used to build a physical picture of the processes operating to produce the deformation. These curves are usually obtained by conducting experiments involving various extensometry techniques [7], but in most cases researchers derive the true curves from the measurement of load vs. elongation, often referred to as an “engineering” curve.

In the case of highly irradiated metals, however, the experimentally recorded “engineering” curves can not always be converted into true curves. This problem arises from the fact that the local flow stress in irradiated metals often develops very specific peculiarities. As a result of irradiation, the metal loses its ability to deform uniformly under tension. A large portion of the highly irradiated specimen does not develop any significant deformation, while the local deformation in the neck area can be very high. In such cases, the engineering curve is inapplicable for studying the kinetics of the deformation processes and, in particular, for defining the character of the relationship between the true stress and strain values.

To obtain an understanding of the events happening in a deforming specimen and, in particular, to study the relationship between the true stresses and strains, one can use special extensometer

* Pacific Northwest National Laboratory (PNNL) is operated for the U.S. Department of Energy by Battelle Memorial Institute under contract DE-AC06-76RLO-1830.

techniques during mechanical testing, such as: optical and electron extensometry [8, 9], coordinate network techniques [10], and speckle-interferometry techniques [11].

When radioactive materials are being tested, the use of these extensometry techniques become much more difficult, often limiting their applicability. For very small or “miniature” specimens used to reduce the level of radioactivity, any technique involving physical or close contact of either measurement probes or persons to the specimens often becomes rather impractical. To overcome such problems we have applied a “marker-extensometry” technique that is uniquely suited to examining very small, highly radioactive specimens that are prone to flow localization on a rather small scale.

Materials Under Study

The study was performed on four pure metals – copper, nickel, molybdenum and Armco-iron. Also were examined Russian industrial alloys 12Cr18Ni10Ti and 08Cr16Ni11Mo3, which are widely used in nuclear reactors in the countries of the former Soviet Union. The compositions of these Fe-base alloys are Cr:18%, Ni:10.6%, Mn:1.7%, C:0.1% and Cr:16%, Ni:11.4%, Mn:1.6%, Mo:1.8% C<0.021%, respectively.

Two types of specimens were used in this study. Flat specimens (See Fig.1a) with gauge section dimensions of 10×3.5×0.3 mm were punched from strips of pure nickel, iron or molybdenum. The specimens were annealed and then irradiated over a range of doses in the core of the WWR-K reactor (located in Almaty, Kazakhstan Republic) to a maximum fluence of 6×10^{20} n/cm² (E > 0.1 MeV). Round tensile specimens (See Fig.1b) of pure copper and 12Cr18Ni10Ti with gauge section 10 mm long and 1.7 mm diameter were also irradiated in WWR-K. All irradiations proceeded over a rather narrow range of temperature but never exceeded 353K.

Additionally, flat specimens of 08Cr16Ni11Mo3 steel with gauge section dimensions of 10×2×0.3 mm were sliced from various axial positions of the faces of the spent fuel assembly wrapper designated H-214(II) that was irradiated in the BN-350 fast reactor in Aktau, Kazakhstan Republic. The damage dose rate and the accumulated dose in this assembly varied along its height. At its centerline a maximum of 15.6 dpa was reached. Unlike the WWR-K data the irradiation temperature of various specimens varied somewhat, ranging from 553 to 600K.

The thermal treatment of the materials and their irradiation conditions are given in Table 1.

Table 1. Thermal treatment and irradiation parameters of the materials under study

Material	Thermal treatment	Irradiation temperature (K), reactor.	Fluence (n/cm ² , E>0.1 MeV) or dose (dpa)
Nickel	Annealing 1223 K, 30 min.	<353, WWR-K	1.4×10^{19} - 1.3×10^{20}
Armco-iron	Annealing 1223 K, 30min.	<353, WWR-K	5×10^{18} - 1.4×10^{19}
Molybdenum	Annealing 1473 K, 2 hours	<353, WWR-K	1.1×10^{19} - 6×10^{20}
Copper	Annealing 1023 K, 1 hour	<353, WWR-K	2×10^{20}
Steel 12Cr18Ni10Ti	Annealing 1323 K, 30 min.	<353, WWR-K	1.4×10^{19} - 1.3×10^{20}
Steel 08Cr16Ni11Mo3	Cold-work 15-20 % + annealing 1073 K, 1 hour.	553-600, BN-350	1.27 - 15.6 dpa

Uniaxial tensile tests of both non-irradiated and irradiated specimens were performed using the “Instron-1195” facility at 293K with a deformation rate of $8.4 \cdot 10^{-4}$ s⁻¹. Pneumatic grippers were used for gripping of the specimens.

Details of the “marker-extensometry” technique

To study the kinetics of non-homogeneous deformation of highly irradiated miniature specimens, a “digital marker extensometry” technique was developed. Small drops (0.3-0.5 mm) of dye material from a marking pen were manually applied to the polished specimen surface. The dye was chosen because it demonstrated good adhesive properties and because it deformed easily without debonding. Note, however, that the use of this dye limits the temperature of the experiment to <373K. Because of the small specimen size, the marker dots and their spacing represent our current limit and thereby the spatial resolution of localized deformation areas.

The shape changes of the specimen, as well as the shape change and shift in position of the markers were recorded by digital camera with high resolution (2048×1536 pixels with a resolution of 10 micron/pixels), as shown in Figure 1.

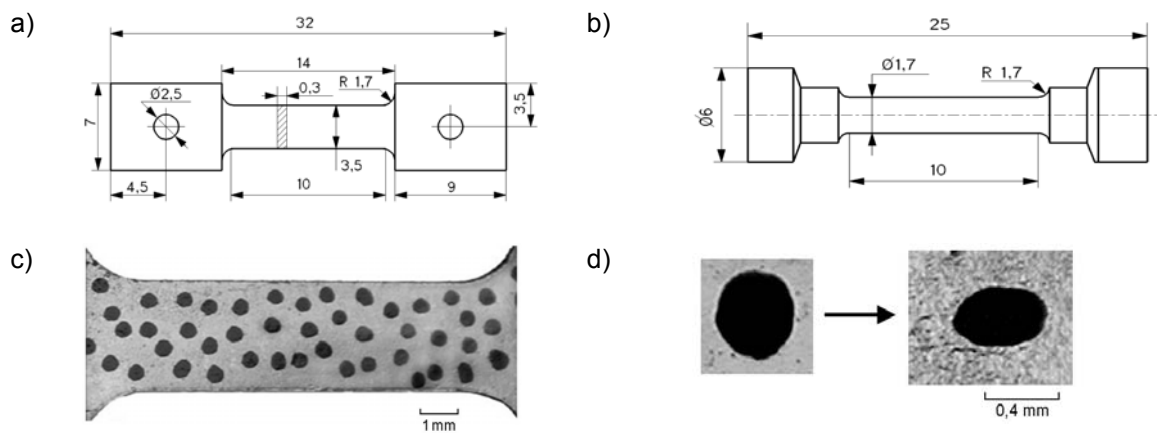


Figure 1. Shape and dimensions in mm of flat (a) and round (b) samples, gauge area of flat specimen before deformation (c) and change of the shape of a single marker as a result of deformation (d).

The easily reproducible and relatively large size markers used in the first cycle of our experiments were chosen as the first stage of development. Later, when more specific algorithms to process the digital images have been established and a stronger optics system has been developed, it will be possible for other, smaller image elements (smaller dots, small scratches, etc) to serve as markers.

In the current marker extensometry technique, which is similar to the “network technique” [10], the specimen is covered with a spot network with steps of 1-1.5 mm. This allows us to calculate the values of local strain and stress with an error not higher than 5 and 10 %, respectively, for any section of the specimen based on a sequence of pictures, using specially developed computer codes that calculate the distance L between the centers of the markers (see Figure 2). The value of the local strain of some chosen local section of the specimen for the i -th picture may be defined as $\varepsilon_i = (L_0 - L_i) / L_i$, where L_0 is the initial distance between the markers (defined from the first picture taken before the deformation started), and L_i is the current distance calculated based upon the i -th picture.

It is a well known fact that the material density ρ does not change much in the process of deformation ($\Delta\rho < 1\%$). This fact allows us to say that the volume of the specimen V can be considered as constant during the course of a tensile experiment.

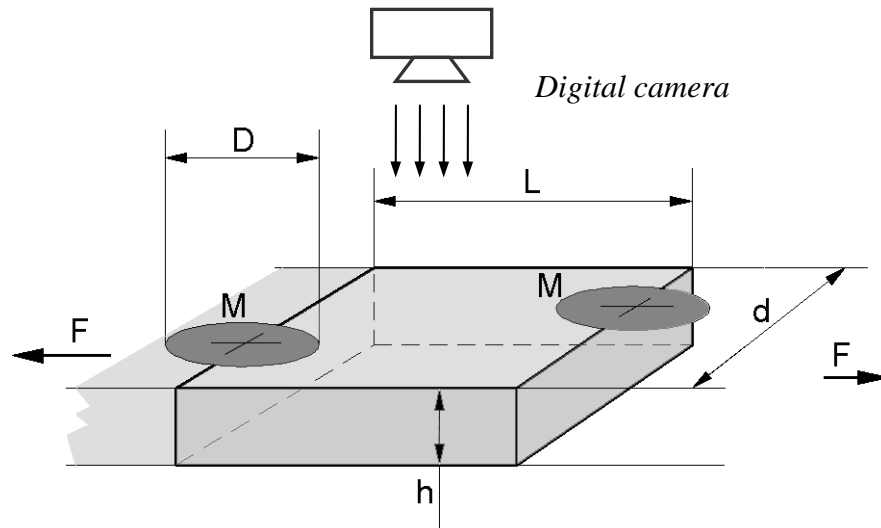


Figure 2. The parameters that are being measured using the marker extensometry technique. The specimen is loaded by the force F . The highlighted section, which has two markers (M); D is the marker's dimension towards the tensile axis; L is the distance between the centers of the markers; d is the width of the specimen; h is the thickness of the specimen (d and h values are defined before the deformation).

Thus, the operating stress σ_i may be obtained based on the constant volume criterion V where ($V=S_0 \cdot L_0 = S_i \cdot L_i = \text{const}$, where $S=h \cdot d$) as follows:

$$\sigma_i = \frac{F_i}{S_0 \cdot \left(\frac{L_0}{L_i} \right)} \quad (1)$$

F_i is the force acting at i -th moment of time and is defined from the engineering diagram, S_0 is initial cross section. The marker dimension along the D axis might be used instead of the L value in the calculations.

This approach allows us to define the stress value acting along the deformation axis but it does not provide an opportunity to define tangential stresses. This paper does not address the analysis of the complex stress state that takes place in the neck region as it develops.

As discussed earlier [7, 8], it is important to note that the method proposed here cannot be used when strain is concentrated in areas smaller than the size of a marker. In addition, at very levels of local strain the "constant volume criterion" will cease to be valid.

Using the experimental values of the true stresses σ_i and the local strain ε_i , one can construct the distribution curve along the operating length of the specimen for various increments of the deformation until failure or to observe the " $\sigma_i - \varepsilon_i$ " relationship for some section of the specimen (see Figure 3).

It is worth noticing that the experimental " $\sigma_i - \varepsilon_i$ " relationships for the irradiated materials [12] are rarely mentioned in the literature. In particular this is true for specimens with high levels of radiation embrittlement. However, the " $\sigma_i - \varepsilon_i$ " curves have great practical value, especially when used in simulation of plastic deformation in calculations using the ANSYS, ABAQUS or LS-DYNA finite element codes.

Experimental Results

08Cr16Ni11Mo3 Steel irradiated in BN-350

Figure 3 shows typical engineering curves obtained through deformation of neutron irradiated 08Cr16Ni11Mo3 steel. The general features of the curves are similar to that of an earlier study [13]. The yield and ultimate stress values and the plasticity obtained from these diagrams, agree well with the results of others [13, 14, and 15]. As seen in Figure 3, the uniform deformation value is very small (2-4%), and immediately after the yield strength one can observe the development of a neck and the engineering curve becomes non-informative concerning the work hardening processes within the neck area. From the scientific point of view it is informative to study the " $\sigma_i - \varepsilon_i$ " relationship in the developing neck (see Figure 3, curves 3 and 3'). The true curve (3') was calculated for the developing neck based on experimental results using the optical extensometer method.

Figure 4 shows the deformation hardening curves for the 08Cr16Ni11Mo3 steel in the "true stresses σ_i – local strain $(\varepsilon_i)^{0.5}$ " coordinates, which were calculated based on the digital marker extensometry data. The square root of strain is used, which according to the suggestion of reference [16] results in linearization of the curves.

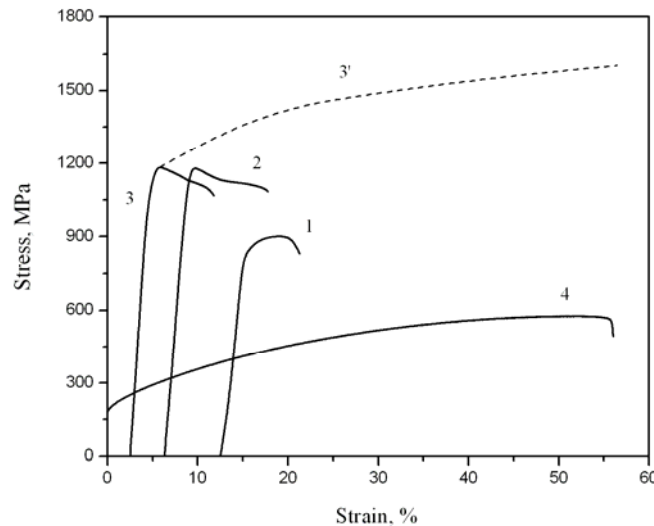


Figure 3. Engineering curves for 08Cr16Ni11Mo3 steel presented in conventional coordinates: 1 – irradiated to 1.27 dpa at 280 °C; 2 – 10.8 dpa at 300 °C; 3 – 11.9 dpa at 354 °C; 3' – the true curve of the plastic flow for curve 3; 4 – non-irradiated steel. The various curves are shifted arbitrarily along the strain axis to provide a better view.

As one can see from comparing Figures 3 and 4, the transition from conventional to real deformation and stress values qualitatively changes the view of the flow curves. Thus, the development of the local strain in the neck is accompanied by continual deformation hardening of the material. The operating stresses increase up to the moment of failure, despite the seeming loss of hardening which is registered by the engineering curve immediately after the yield point. According to [17], here we see the "quasi-embrittlement" case, i.e. the suppression of the uniform deformation, and, this case should be differentiated from that of real embrittlement [18], i.e. the complete suppression of the material's capability for plastic deformation.

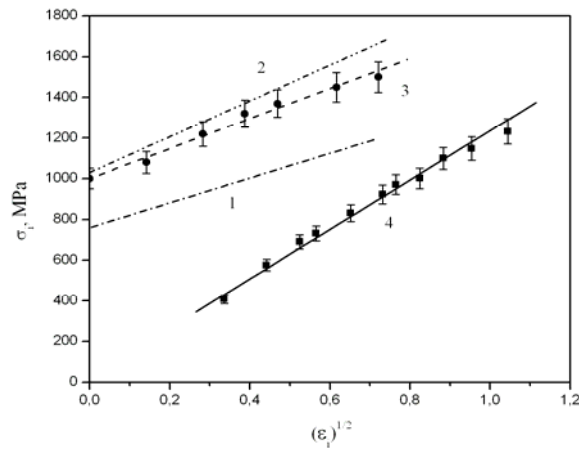


Figure 4. The “true stress σ_i – local strain $(\varepsilon_i)^{0.5}$ ” relationship for 08Cr16Ni11Mo3 steel. Curves 1-4 correspond to the specimen numbers shown in Figure 3. The experimental data points are not shown for curves 1 and 2.

Analysis of the experimentally obtained $\sigma_i(\varepsilon_i)$ relationships showed that they may be described by the following equation:

$$\sigma_i = k \cdot \varepsilon_i^{0.5} + \sigma_0, \quad (2)$$

where k is the coefficient of the strain hardening and σ_0 is a value close to the yield strength. In “ $\sigma - \varepsilon^{0.5}$ ” coordinates these curves appear to be linear.

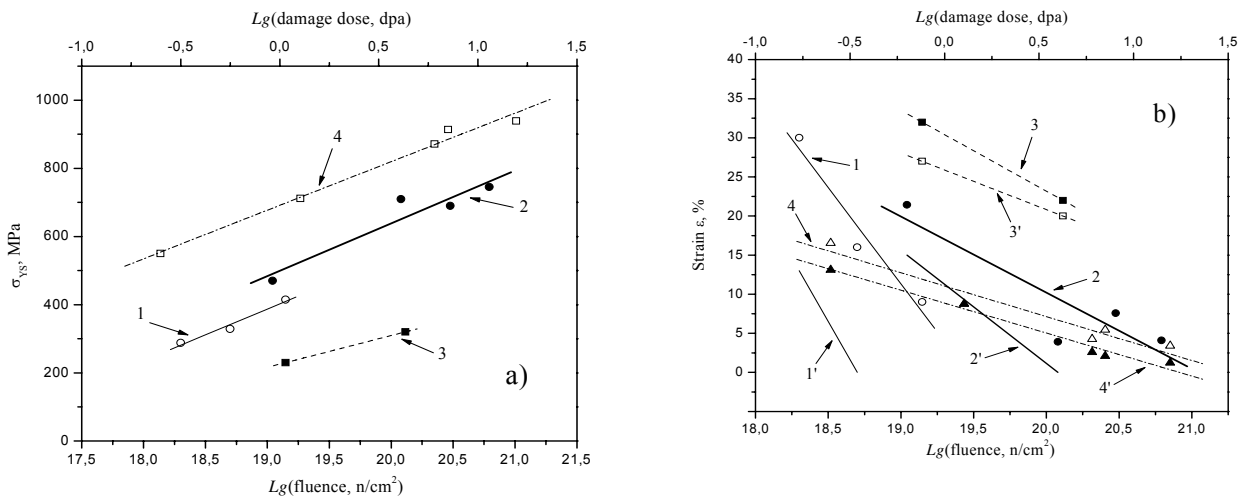


Figure 5. Changes in yield strength (a) and plasticity (b) versus fluence (for Fe, Ni, Mo) or damage dose (for steel 08Cr16Ni11Mo3): 1 – α -Fe, 2 – Mo, 3 – Ni, 4 – 08Cr16Ni11Mo3 steel. 1-4 – total and 1'-4' – uniform deformation for the indicated materials.

In this steel we observe monotonic growth of the σ_0 value with increasing dose, while the k value in general decreases but not monotonically. To explain this non-monotonic behavior we speculate that in addition to the dose level, factors such as differences in irradiation temperature and dose rate in this data set affect the material's structure and its deformation behavior [19].

Pure metals (Cu, Fe, Ni, Mo) and 12Cr18Ni10Ti stainless steel irradiated in WWR-K

Figure 5 shows strength and plastic engineering properties of the pure metals versus neutron fluence. In this figure one can see that the yield strength of these metals is steadily increasing, while the plasticity is decreasing. The data agree well with data from other studies [20].

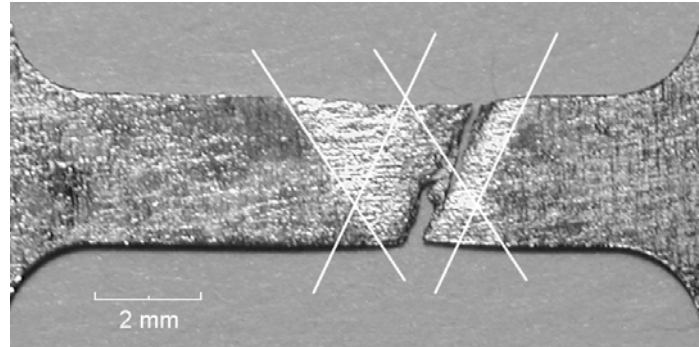


Figure 6. Localized deformation and neck formation in molybdenum irradiated by neutrons to 3×10^{20} n/cm².

The decrease in plasticity demonstrates itself most vividly in the bcc metals, for which the uniform deformation values plunges toward zero when the fluence reaches 1.2×10^{20} n/cm² for molybdenum and 1.4×10^{19} n/cm² for iron. Similar to the case of the steel irradiated to > 10 dpa, the uniform deformation value defined from the engineering diagrams does not exceed 4-6%, in agreement with data in [20, 21, 22]. These specimens lose their ability to deform uniformly and plastic flow becomes concentrated in a very narrow area (see Figure 6) which is usually located in the vicinity of one of the grippers. There are only a few cases when two areas of localized deformation develop. It is quite clear that in this situation the engineering diagrams are of little value to study the plastic flow of the irradiated material.

Figures 7-9 show the engineering and true tensile curves obtained for the various metals. Following suggestions in [16] and also for convenience, we continue to use the square root of the local strain value of the “ $\sigma_i - \varepsilon_i$ ” curves. Once again linearization of the “ $\sigma_i - \varepsilon_i$ ” curves occur and can be described by the equation $\sigma_i = \sigma_0 + k\sqrt{\varepsilon_i}$.

Comparing the two types of pictures, one can see that the transition from the engineering to the true curve highlights a qualitative change in the nature of the curve. The concept of ultimate strength does not appear to be applicable since hardening continues in the deforming area up to the failure of the specimen. The local strain may reach values that exceed values obtained from the engineering diagrams by at least 1.5 to 2 times.

Analyzing these experimental data one may assume that the “ $\sigma_i - \varepsilon_i$ ” curves allow us to obtain more reliable information on the kinetics of the deformation processes and on some peculiarities of interactions of dislocations and radiation defects compared to that obtained from the engineering curves. Table 2 presents the values of K and σ_0 obtained from these studies. In particular, from the true curves it is seen that the σ_0 value continually increases with increasing fluence while the hardening coefficient does not change significantly.

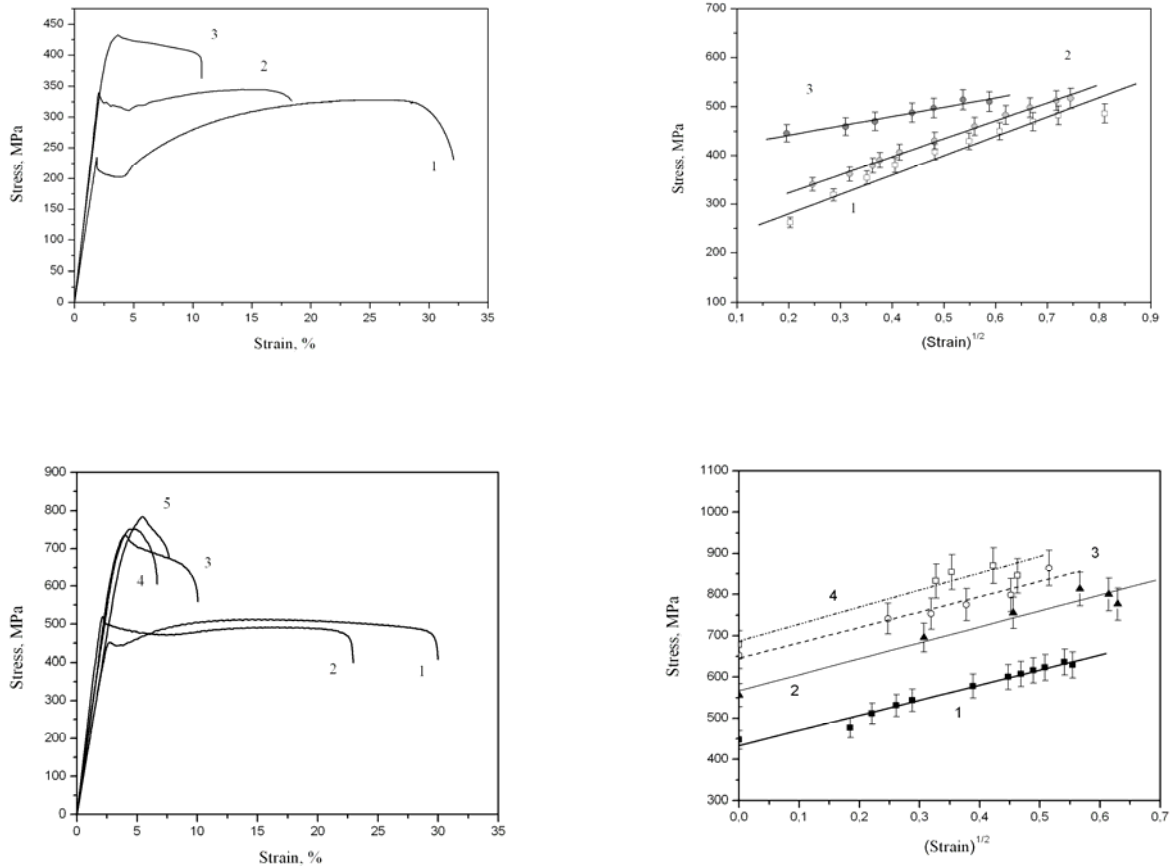


Figure 7. Engineering “stress – strain” curves and “ $\sigma_i - \epsilon_i$ ” relationships for non-irradiated and neutron irradiated bcc materials. On the top: Armco-iron, 1 – non-irradiated specimen, 2 – 5×10^{18} n/cm², 3 – 1.4×10^{19} n/cm². On the bottom: molybdenum, 1 – non-irradiated; 2 – 1.1×10^{19} n/cm²; 3 – 1.2×10^{20} n/cm²; 4 – 3×10^{20} n/cm²; 5 – 6.2×10^{20} n/cm².

Table 2. Values k and σ_0 obtained for unirradiated and irradiated materials.

Material	Fluence (n/cm ²) or damage dose (dpa)	Yield stress σ_{02} , MPa	σ_0 , MPa	k , MPa
Steel Cr18Ni10Ti	0	200	180	830
Steel Cr18Ni10Ti	1.4×10^{19}	510	480	790
Steel Cr16Ni11Mo3	15.6 dpa	920	1100	690
Ni	–	59	85	587
Ni	1.4×10^{19}	236	205	470
Ni	1.4×10^{19}	316	265	448
Fe	–	202	215	369
Fe	5×10^{18}	311	250	369
Fe	1.4×10^{19}	399	405	192
Cu	–	50	13	438
Cu	5×10^{20}	350	259	110

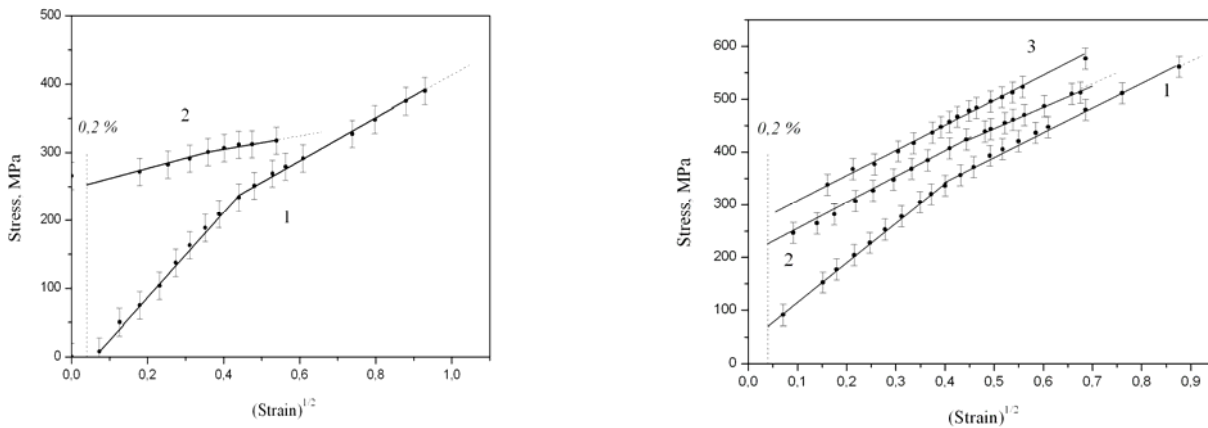


Figure 8. “ $\sigma_i - \varepsilon_i$ ” relationships for non-irradiated and neutron irradiated copper (at the left, 1 – non-irradiated specimen, 2 – 2×10^{20} n/cm²) and nickel (at the right, 1 – non-irradiated specimen, 2 – 1.4×10^{19} n/cm²; 3 – 1.3×10^{20} n/cm²).

As one can see, the k value for irradiated nickel is smaller than for non-irradiated nickel and at the same time k does not change when the fluence increases from 1.4×10^{19} to 1.3×10^{20} n/cm².

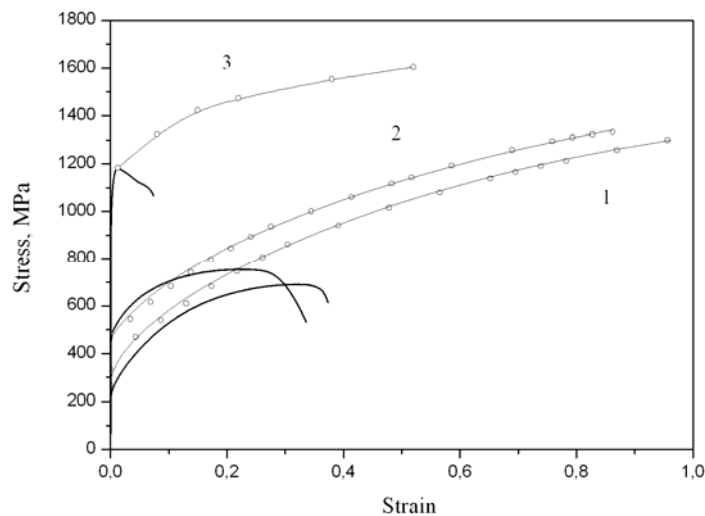


Figure 9. Engineering curves (thick solid lines) and “ $\sigma_i - \varepsilon_i$ ” relationships (with circles) for the non-irradiated (1) and irradiated neutron stainless steels. 2 – 12Cr18Ni10Ti (WWR-K, 1.4×10^{19} n/cm²), 3 – 08Cr16Ni11Mo3 (BN-350, 15.6 dpa).

Another aspect of the marker extensometry method is that it allows visualization of the distribution of strain along the specimen axis. This is particularly useful when the material is just beginning to harden but appears still to be in the uniform elongation regime. Note in Figure 10 that the strain is not uniform along the length of the specimen but appears to indicate some periodicity. This specimen was 12Cr18Ni10Ti irradiated in WWR-K to 1.4×10^{19} n/cm² or ~ 0.01 dpa. This indicates that some areas initiate plastic deformation before others although subsequent strain rates appear to keep pace at all positions. So the term “uniform” elongation is not a completely correct description of the deformation process. Stress concentrations near the two grips might account for two of the initiation sites but not for the other three sites.

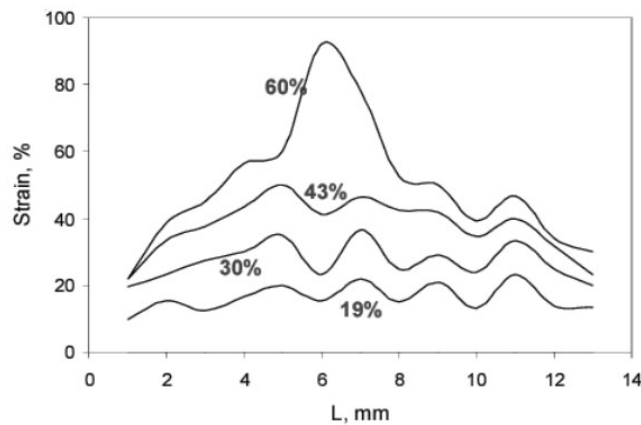


Figure 10. Distribution of strains along the length of 12Cr18Ni10Ti specimen irradiated in WWR-K to 1.4×10^{19} n/cm², taken at equal time intervals during the tensile test. The percentages shown are the elongation observed in the engineering curve.

Figure 11 demonstrates that until necking begins to occur the various regions exhibit identical local strain behavior, following the same true “stress-strain” curve. When the ultimate stress is reached, however, necking occurs and the non-necking areas drop out of the deformation process. The true stress decreases and plastic flow stops in these bypassed areas.

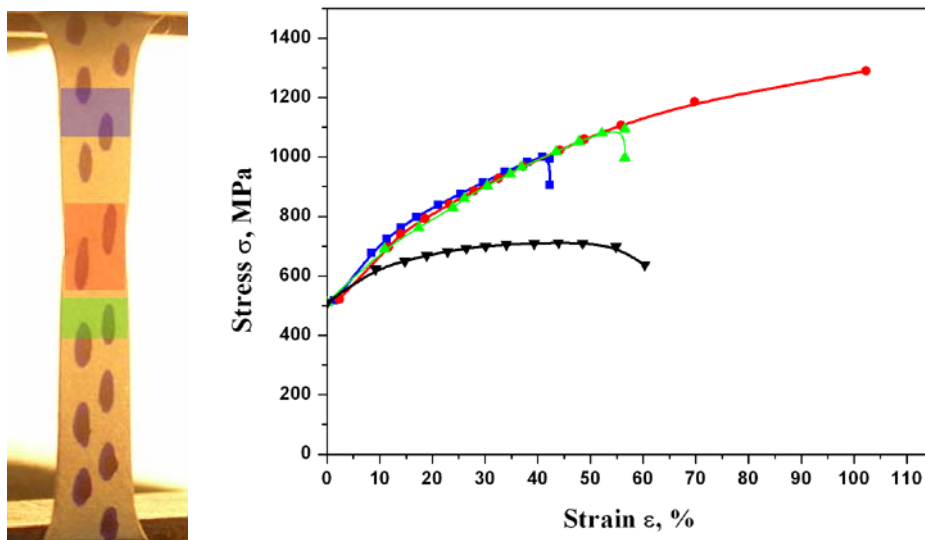


Figure 11. Comparison of engineering (black) and true strain curves (designated by colors) for three areas, showing that all three follow the same true curve initially, but as necking develops the other areas drop out of the deformation process.

Conclusions

To study the peculiarities of the deformation hardening and flow localization of radioactive materials, a non-contact “digital marker extensometry” technique has been developed. It allows the researcher to easily define plasticity parameters and true stresses in experiments where highly radioactive miniature specimens are used.

The “ $\sigma_i - \epsilon_i$ ” relationship during plastic flow and hardening of irradiated metal polycrystals has been investigated experimentally. True curves have been obtained for nickel, iron, molybdenum, as well as for the 08Cr16Ni11Mo3 and 12Cr18Ni10Ti steels. Describing these curves using the

$\sigma_i = \sigma_0 + k\sqrt{\varepsilon_i}$ equation demonstrates that the concept of ultimate stress is an artifact arising from flow localization and is not fully informative of the hardening mechanisms operating in highly irradiated materials.

Acknowledgements

This work was conducted in Kazakhstan under ISTC K-437 Research Contract and "Government Fund of Fundamental Research of Kazakhstan Republic". The participation of F. A. Garner was sponsored by the US department of Energy, Office of Fusion Energy under Contract DE-AC06-76RLO 1830 at Pacific Northwest National Laboratory.

References

- [1] G. A. Malygin, "Structural factors which affect the stability of plastic deformation during a tensile test of bcc metals", *Solid State Physics*, 2005, Vol. 47, Issue 5, pp. 870-875 (in Russian).
- [2] G. A. Malygin, "Analysis of the structural factors responsible for formation of the bottle neck area during tensile testing of fcc metals and alloys", *Solid State Physics*, 2005, Vol. 47, Issue 2, pp. 236-241 (in Russian).
- [3] V. S. Ivanova, "Synergetics: Strength and failure of metal materials", Moscow, 1992.
- [4] V. E. Panin, A. D. Korotayev, P. V. Makarov, V. M. Kuznetsov, "Physical mezosmechanics of materials", *Institute Newsletter: Physics*, 1998, № 9, pp. 8-37 (in Russian).
- [5] M. M. Krishtall, "The instability/mesoscopic non-uniformity interaction of plastic deformation; Part 2, The non-linear model of the plastic deformation stability: the build-up, analysis, numerical simulation and quantitative estimates", *Physics of Metals and Material Science*, 2001, Vol. 92, Issue 3, pp. 96-112 (in Russian).
- [6] G. A. Malygin, "Analysis of the factors causing the instability of deformation and loss of plasticity for neutron irradiated copper", *Solid State Physics*, 2005, Vol. 47, pp. 632-638 (in Russian).
- [7] O. P. Maksimkin, M. N. , Gusev, I. S. Osipov, "Deformation extensometry during mechanical tests of highly radioactive metal and alloy specimens", *Information News of the National Nuclear Center of the Republic of Kazakhstan*, 2005, Issue 1, pp. 46-52 (in Russian).
- [8] A. A. Babushkin, O. P. Maksimkin, S. Y. Chelnokov, "Optical-electron extensometer". Publications of the Academy of Sciences of Kazakhstan, *Physics & Mathematics Series*, 1986, № 2 (in Russian).
- [9] C. Brillaud, T. Meylogan, P. Salathe, "Use of laser extensometer for mechanical tests on irradiated materials", *Effect of Radiation on Materials: 17th International Symposium*, ASTM STP 1270, 1996, p. 1144.
- [10] B. A. Migachev, V. P. Volkov, "Enhancement of the measuring precision technique of the deformation state using coordinate networks", *Factory Laboratory*, 1988, Vol. 54, № 5 pp. 77 (in Russian).
- [11] V. V. Gorbatenko, S. S. Polyakov, L. B. Zuev, "Visualization of local deformation areas using calculational de-correlation of video images with a speckle-structure.", *Factory Laboratory. Material Diagnostics*, Vol.67, № 7, 2001, pp. 29-31 (in Russian).
- [12] T. S. Byun, and K. Farrell, "Plastic instability in polycrystalline metals after low temperature irradiation", *Acta Materialia*, Vol. 52, Issue 6, 5 April 2004, pp. 1597-1608.
- [13] M. G. Horsten, M. I. De Vries, "Irradiation hardening and loss of ductility of type 316l(n) stainless steel plate material due to neutron-irradiation", *Effect of Radiation on Materials: 17th International Symposium*, ASTM STP 1270, 1996, p. 919.
- [14] M. L. Hamilton, F. A. Garner, G. H. Hankin, R. G. Faulkner, M. B. Toloczko, "Neutron-induced evolution of mechanical properties of 20% cold-worked 316 stainless steel as observed in both miniature tensile and tem shear punch specimens", *Effects of Radiation on Materials: 19th International Symposium*, ASTM STP 1366, M. L. Hamilton, A. S. Kumar, S. T. Rosinski and M. L. Grossbeck, Eds., American Society for Testing and Materials, 2000, pp. 1003-1017.
- [15] I. V. Gorynin, Vinokurov, et al., "A comparative evaluation of the operational characteristics of austenitic class steels with respect to the operational conditions of the ITER discharge chamber", *A Collection of works on "Radiation effects on the fusion reactor materials"*, C-P6, September 21-24, 1992, pp. 90-109 (in Russian).
- [16] V.I. Trefilov, V. F. Moyiseev, and others, "Deformation hardening and failure of polycrystal metals", Kiev, "Naukova Dumka", 1989, p. 256 (in Russian).

- [17] G. A. Malygin, "Analysis of the structural factors causing formation of necking during tensile tests of metals and fcc alloys", *Solid State Physics*, 2005, Vol. 47, Issue 2, p. 236 (in Russian).
- [18] F. A. Garner, Chapter 6: "Irradiation performance of cladding and structural steels in liquid metal reactors", V.10A of *Materials Science and Technology: A Comprehensive Treatment*, VCH Publishers, 1994, pp. 419-543.
- [19] F. A. Garner, "Demonstration of the separate temperature and dpa rate dependencies of void swelling in 300 series stainless steels", 12th International Conference of Fusion Reactor Materials, Santa-Barbara, December 4-9, 2005, abstract booklet, p. 334.
- [20] A. M. Parshin, "Structure, strength and radiation damage of corrosion resistant steels and alloys", Chelyabinsk, "Metallurgy", Chelyabinsk branch, 1988, p. 656 (in Russian).
- [21] V. S. Neustroev, E. V. Boev, F. A. Garner, "Low temperature mechanical properties of Fe-0.06C-18Cr-10Ni-0.4Ti austenitic steel determined using ring-pull tensile tests and microhardness measurements", *J. Nucl. Mater.* 367-370, 2007, pp. 935-939.
- [22] O. P. Maksimkin, "Phase-structure processes and their role in hardening and embrittlement of irradiated metal materials", Doctor's of Physics and Mathematics, Scientific Thesis, Almaty, 1996 (in Russian).